ISSN 1810-2328, Journal of Engineering Thermophysics, 2018, Vol. 27, No. 3, pp. 345–356. © Pleiades Publishing, Ltd., 2018.

The pH Effect on Thermal Response of Fluorescence Spectroscopy of Graphene Quantum Dots for Nanoscale Thermal Characterization

Ch. Li[1], J. Zhang[2], Q. Xiong[3], G. Lorenzini[4], and Y. Yue[1]*

[1]*School of Power and Mechanical Engineering, Wuhan University, Wuhan, Hubei, 430072 China*

[2]*Holland Computing Center, University of Nebraska-Lincoln, Lincoln, NE, 68588 USA*

[3]*Oak Ridge National Laboratory, Oak Ridge, TN, 37831 USA*

[4]*Dipartimento di Ingegneria e Architettura, Università degli Studi di Parma, Parma, 43124 Italy*

Received January 18, 2016

Abstract—Accurate and sensitive nanoscale thermal probing for thermophysical property characterization is appealing but still a challenge to date. Previous studies have revealed that graphene quantum dots (GQDs) are good temperature markers for their small dimension and superior fluorescence excitation. In this work, we show that the thermal response of fluorescence spectrum of GQDs is strongly pH-dependent. Significant decrease (about 56% to 30%) for temperature-induced intensity reduction within a small range of 75°C under different excitation wavelengths of 370 nm, 390 nm, and 410 nm is observed as pH value increases from pH = 1 to pH = 13. The temperature coefficients of peak wavelength change from positive to negative with the increase of pH value, meaning that the blue shift happens as the condition is changed from acidity to alkalinity. Temperature dependence of peak width is also studied with the largest coefficient of 0.2255nm/°C, which is remarkable. These suggest that when using GQDs in nanoscale thermal probing, the pH value is an important factor that should be considered besides the excitation wavelength. Regarding the superior biocompatibility and low cytotoxicity, GQDs could play an important role in thermal probing or mapping in a complex biology system such as a cell, and help to develop novel treatments and diagnoses.

DOI: 10.1134/S1810232818030104

1. INTRODUCTION

Quantum dots (QDs) exhibit unique and tunable optical and electronic properties arising for their small dimension and large surface-to-volume ratio (A/V) [1–3]. Great efforts have been devoted to the development of advanced synthetic methods and multi-disciplinary applications [4–7]. For example, they can be used in bioimaging for their high quantum yields and resistance to photobleaching, and the continuous and strong optical absorption profiles [8–12]. Besides, they show great potentials in energy conversion for the large charge mobility and absorbing property [13–20], and can be assembled as industrial sensors [21–26]. Among many applications, one appealing implementation is to use QD as a temperature sensor by employing exceptional fluorescence excitation characteristics [27–29]. Combined with the temperature dependence of fluorescence spectroscopy and the nanoscale size, QD can be developed as an excellent probe for nanoscale thermal sensing and mapping [30–32].

In thermal imaging application, it is desirable to find one material exhibiting excellent temperature sensitivity while keeping the stable optical property [33]. Fluorescence spectroscopy methods have shown great potential in the areas of nanoscale thermal probing/imaging [34, 35]. In our previous study, we found that graphene quantum dots (GQDs) have excellent temperature dependence of their fluorescence signal: the intensity of fluorescence signal drops by 50% within a small room temperature range of 75°C [36]. The GQDs are fragments of graphene, which reserve the excellent property of

*E-mail: yyue@whu.edu.cn

graphene meanwhile behave new characteristics as being QDs. As the development of synthesis methods, large-scale production of GQDs becomes available [37]. Considering their bio-compatible characteristics, GQDs are very promising in bio-thermal imaging down to nanoscale. It is well known that the temperature dependence of fluorescence of QDs can be affected by the sample size [38, 39], which is the same for GQDs. Other experimental conditions, such as excitation wavelength, impact the quantum efficiency, which may vary for different samples sizes. Therefore, it is essential to explore the thermal response of fluorescence characteristics to different conditions/parameters, and further to interpret the physical mechanism for the spectrum phenomenon.

During synthesis of GQDs, the pH value is an important parameter to determine the characteristic of the sample. In application scenario, the GQDs could be used and characterized in different environment with different pH value. Therefore, it is important to consider the effect of pH value on fluorescence excitation, and thus on temperature sensing performance. Taking biology thermal imaging as an example, the biochemical reactions exist in complicated cellular environment, accompanied with heat generation as unutilized energy is discharged. Intracellular temperature will be changed and alters the physical state of DNA and proteins [40], in turn, affects the chemical equilibria and energy metabolism. Thus, the local temperature of the living cells could provide us a novel insight about its pathology and physiology [41], which enables unique methods to novel treatment and diagnoses. In the past, various approaches have been proposed to detect cellular temperature [42–47], including the QDs method [43, 44]. The complicated pH environment in a cell could affect greatly the characteristics of QDs [23, 26,

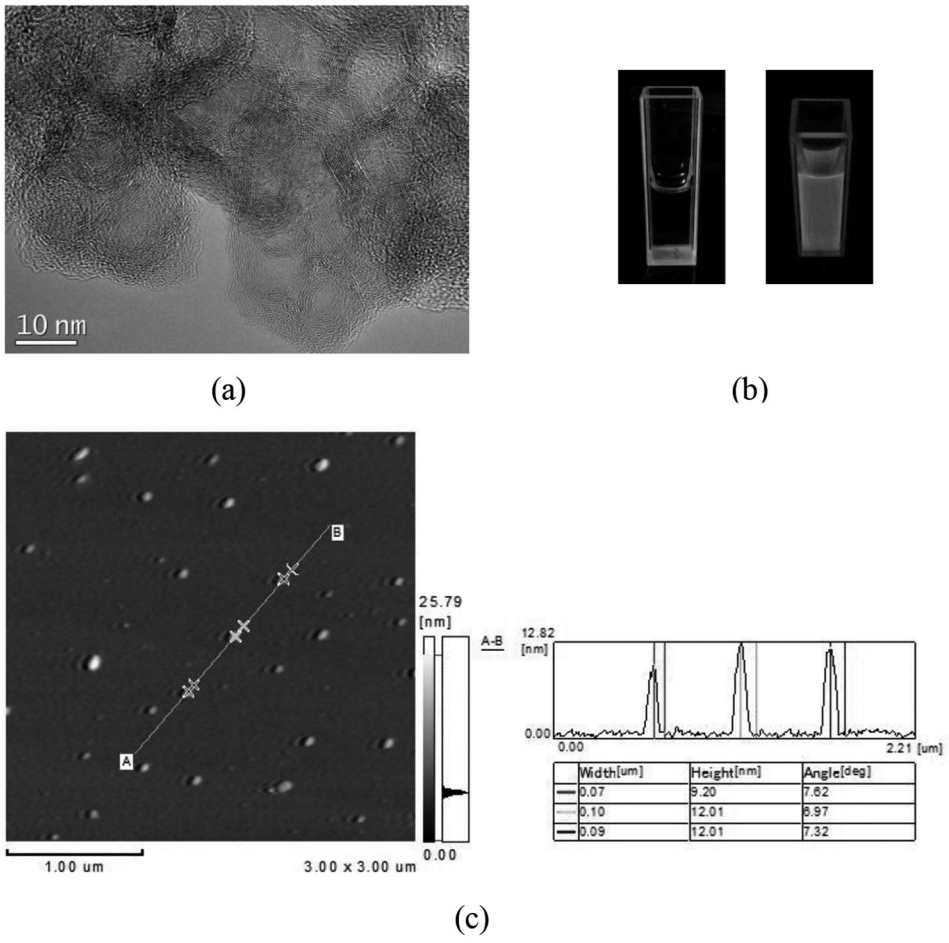

Fig. 1. Characterization of GQDs sample: (a) high-resolution transmission electron microscopy (HRTEM) image (supplied by the company) shows that the GQDs have a uniform diameter of about 10 nm; (b) photos of GQDs aqueous solution under visible light (left) and UV irradiation (right); (c) AFM image of GQDs sample shows that the average thickness of three GQDs selected randomly is about 11 nm.

48–51]. As we have proved that GQD is a good candidate as temperature sensor [36], it would be a great potential for being employed in bio-thermal imaging; thus, we present here an experimental study on the pH effect on the thermal response of fluorescence spectroscopy of GQDs.

2. EXPERIMENTAL DETAILS

A GQD sample was synthesized in Chongqing First Graphene Co., Ltd. by using the bottom-up method [52, 53]. The morphology and size of GQDs were characterized using a high-resolution transmission electron microscopy (HRTEM), as shown in Fig. 1a (provided by the supplier). It shows that the GQDs have a uniform size of 10 nm. Figure 1b presents sample images under visible light (left) and UV beam (right), respectively. The blue luminescence under UV irradiation reveals that the GQDs solution is in good condition for fluorescence excitation. The photoluminescence quantum yield is up to 17%. Figure 1c shows the atomic force microscopy (AFM) image of the GQDs, which was taken on the platform of SHIMADZU SPM-9500J3. The average thickness of three GQDs selected randomly is about 11 nm. The fluorescence experiment was performed on a Horiba Jobin Yvon Fluorolog-3 fluorescence spectrometer. The excitation wavelength can be adjusted from 200 to 1000 nm, and the spectrometer can collect light emission from 300 to 1550 nm. To investigate the effect of pH value on fluorescence of the GQDs, a series of experiments with different pH values under different excitation wavelengths were conducted.

The heating experiments were conducted to study the effect of pH value on the thermal response of fluorescence spectrum. The GQDs sample was adjusted to be at different pH values: pH = 1, pH =7, and pH = 13, for acidity, neutral and alkalinity, respectively. The solution was filled in a sample cell and placed in the T-sample compartment of the fluorescence spectrometer. The fluorescence was first measured at 5°C and then at several temperatures from 5 to 80°C. The temperature was precisely controlled steady with an accuracy of 0.01°C. For each temperature, the sample was maintained for 10 min and three measurements were taken for averaging. The slit width and the integration time were set to 5 nm and 0.1 s for all measurements.

3. RESULTS AND DISCUSSION

3.1. The Effect of pH on Absorption and Excitation Photon Wavelength

Figure 2a is the UV-vis absorption spectrum of GQDs at different pH value, which shows strong optical absorption with the absorption band of $\sim$ 260 nm in the UV region and a tail extending out into the visible range. When the pH value was increased from pH = 1 to pH = 13, little change could be observed in the absorption spectrum, implying that the pH value has little impact on the absorption characteristics. Figure 2b is the fluorescence excitation spectrum with a detection wavelength of 500 nm. It reveals the fluorescence characteristics of GQDs at different pH values. The narrow excitation band at 370 nm in the spectrum of pH = 1 indicates that 370 nm excitation wavelength induces the strongest fluorescence at 500 nm. It needs to be considered that only wavelength falling within this range is suitable when selecting excitation sources. For pH = 7 and pH = 13, relatively broader bands are observed. This phenomenon evidences that the pH value could significantly modify the fluorescence characteristics not just in intensity but also in wavelength. Figures 2c–2e show the fluorescence spectrum of GQDs at different pH values under different excitation wavelengths. For acid environment (pH = 1) as shown in Fig. 2c, the fluorescence peak intensity decreases and the peak shifts toward longer wavelength as the excitation wavelength changes from 370 to 455 nm. This reveals that the fluorescence signal of GQDs in acid solution is more favorable to shorter wavelength light source. As acidity changes gradually to neutral (pH = 7), as shown in Fig. 2d, the fluorescence peaks show no much difference in intensity for different excitation wavelengths. It is noticed by comparing with Fig. 2c that the peak excited by 455 nm light has stronger intensity and narrower peak shape. Similar phenomenon appears in the case for pH = 13: the peak intensity excited under all wavelengths is decreased and the signal doesn't show much difference in intensity among different excitation wavelengths. All of these keep consistent with the sharp peak at pH = 1 and the broad bands at pH = 7 and pH = 13 of the fluorescence excitation spectrum in Fig. 2b. It reveals that fluorescence excitation efficiency can be influenced significantly the pH value. Somehow, it shows a strong selective characteristic in excitation wavelength (e.g., pH = 1 in this case), that is, only short range of light wavelength can effectively excite a fluorescence signal. When the pH value is increased, the excitation band is broadened so that fluorescence signal from

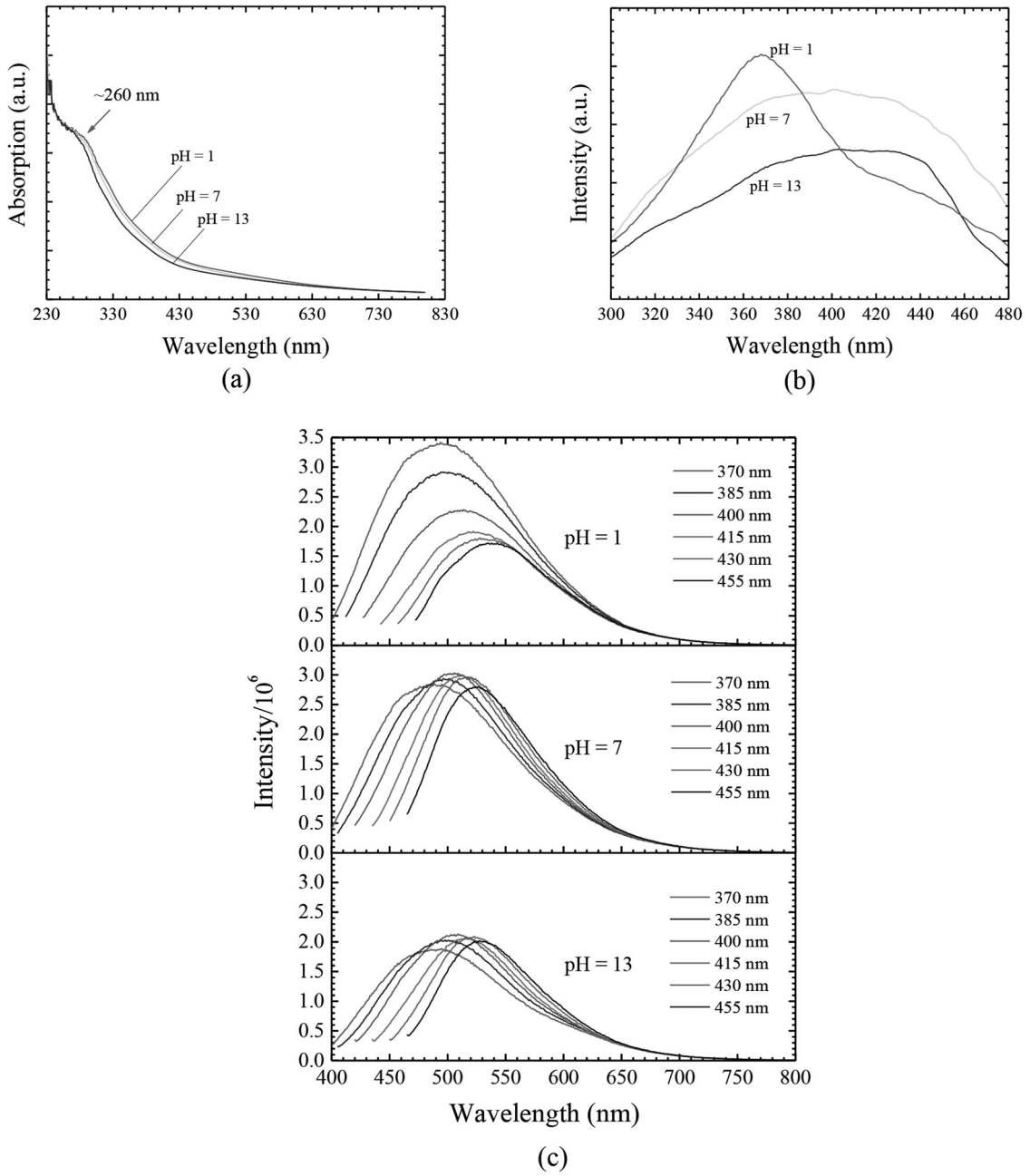

Fig. 2. (a) UV-vis absorption spectra of GQDs with an absorption band of ~ 260 nm are observed at different pH value; (b) fluorescence excitation spectrum with detection wavelength of 500 nm of different pH value. A narrow excitation band at 370 nm for pH = 1 and relatively broader bands for pH = 7 and pH = 13 are observed; (c) fluorescence spectrum of GQDs at different pH value at different excitation wavelengths. The intensity decreases as excitation wavelengths increase from 370 to 455 nm in pH = 1 and changes little in pH = 7 and pH = 13.

excitation wavelength of 370 nm to 455 nm is strong. As pH value is increased, all signals excited by these wavelengths become weak, which can be explained by the shift of excitation band. There are other witnesses of this phenomenon. For example, Deng et al. [49] have found that more trap sites on the CdTe quantum dots surface were removed when the pH value was decreased, this dramatically improved the fluorescence efficiency and stronger fluorescence intensity was observed. Similar results were reported by Gao et al. in the earlier studies [54].

Beside the fluorescence intensity, it is observed that the fluorescence peak position (wavelength, or,

say, the photon frequency) changes for different pH values even under the same excitation wavelength. It means the pH value changes the excited photon wavelength. This peak shift is attributed to the GQDs surface additional reaction caused by different pH values [49, 54, 55]. Yang et al. [51] proposed that GQDs have a triplet ground state carbine-like zigzag edge sites, which can be switched mutually in solution depending on pH value. This makes the fluorescence intensity and wavelength vary reversibly. The above-presented information reveals that the pH value of environmental solution can tune the optical properties of GQDs.

3.2. Effect of pH on Thermal Response of Fluorescence Spectrum

Three different wavelengths (370, 390, and 410 nm) are chosen for fluorescence excitation under different heating experiments, as summarized in Fig. 3. First, the fluorescence spectrum intensity decreases as temperature increases from 5°C to 80°C for all pH values excited with all wavelengths, but the down trend becomes smoother as pH value increases from acidic (pH = 1) to alkaline (pH = 13). Second, the peak position of spectrum changes with temperature increasing and the phenomenon varies with pH values: For pH = 1, the fluorescence spectrum of all different excitation wavelengths shifts to red direction. This temperature-induced red-shift of 370 and 390 nm becomes less obvious as the pH

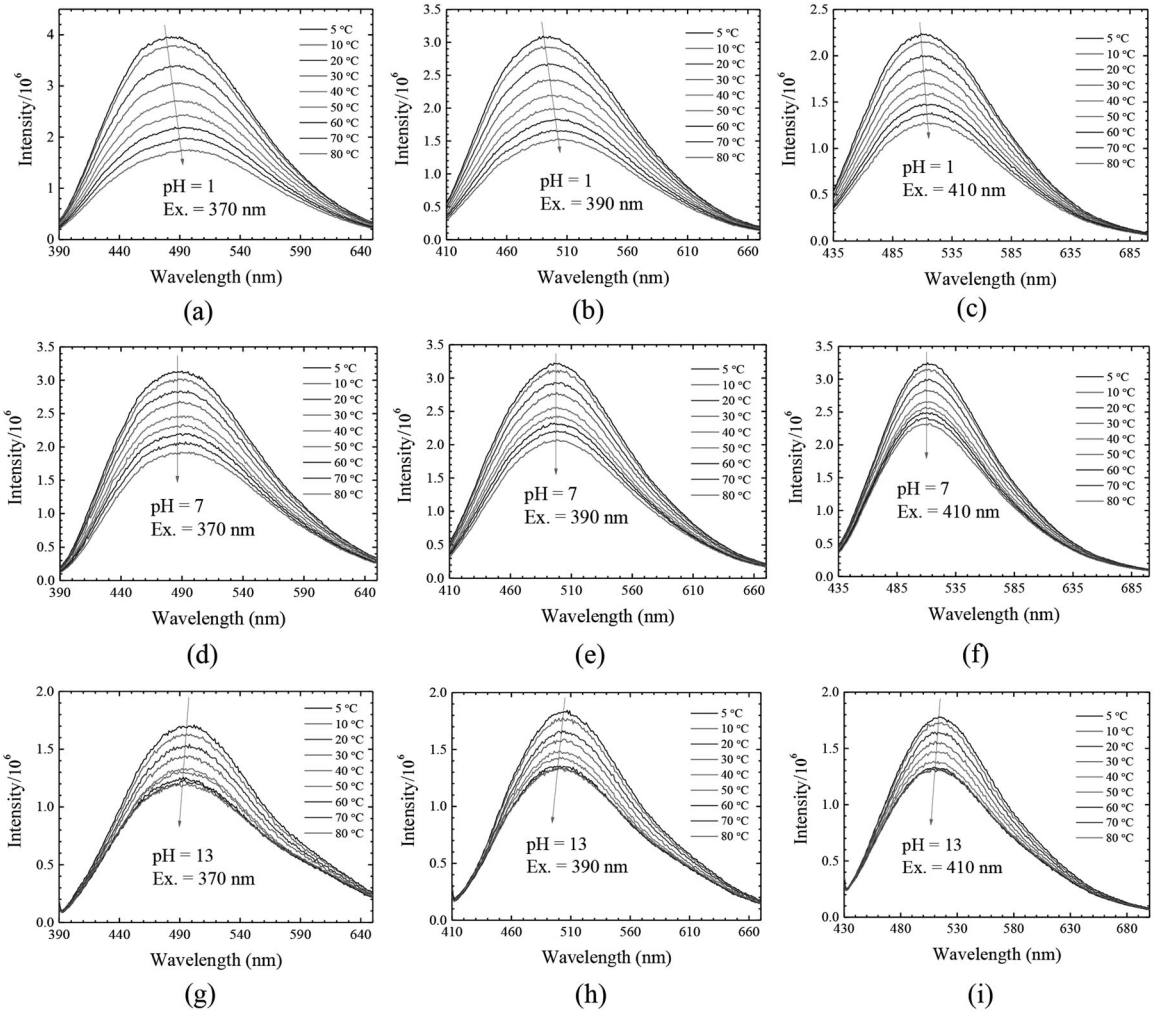

Fig. 3. Temperature dependence of fluorescence spectrum under 370 nm, 390 nm, and 410 nm excitation wavelengths at different pH value. The fluorescence spectrum intensity decreases clearly as temperature increases from 5°C to 80°C for all the excitation wavelengths under different pH value. Temperature-induced red shift of all the wavelengths at pH = 1 (a)–(c) becomes less obvious at pH = 7 (d)–(f), and then changes into blue shift when pH = 13 (g)–(i).

value increased to pH = 7. For an excitation wavelength of 410 nm under pH = 7, no obvious shift is observed, as shown in Fig. 3f. It is worth noting that when the pH value is increased to pH = 13, the corresponding fluorescence spectrum changes into blue-shift with temperature increasing. As usually, a third parameter: the peak width defined as the full width at half maximum (FWHM), no intuitive changes are observed because the fluorescence spectrum of GQDs is broad and asymmetric. In order to understand the mechanism more clearly, we quantitatively analyze the effect of pH on the thermal response of fluorescence spectrum.

3.3. Combined Analysis with Excitation Wavelength

Figures 4a–4c show the quantitative analysis for temperature dependence of fluorescence intensity for three excitation wavelengths. The peak intensities of fluorescence spectrum are normalized by the peak intensity at the lowest temperature (i.e., 5°C). To make clearer, Fig. 4d lists all the temperature-induced intensity reduction of different excitation wavelengths of 370 nm, 390 nm, and 410 nm at different pH values. Figure 4d shows that the intensity reduction for the temperature range of 75°C of all of the excitation wavelengths decreases as the pH value increases from pH = 1 to pH = 13. In the figure of pH = 1 (Fig. 4a), there is around 56% decrease within the temperature range of 75°C under an excitation wavelength of 370 nm, similar to the previous work [36]. The intensity reduction decreases as the excitation wavelength changes from 370 nm to 410 nm, but still about 43% when the excitation

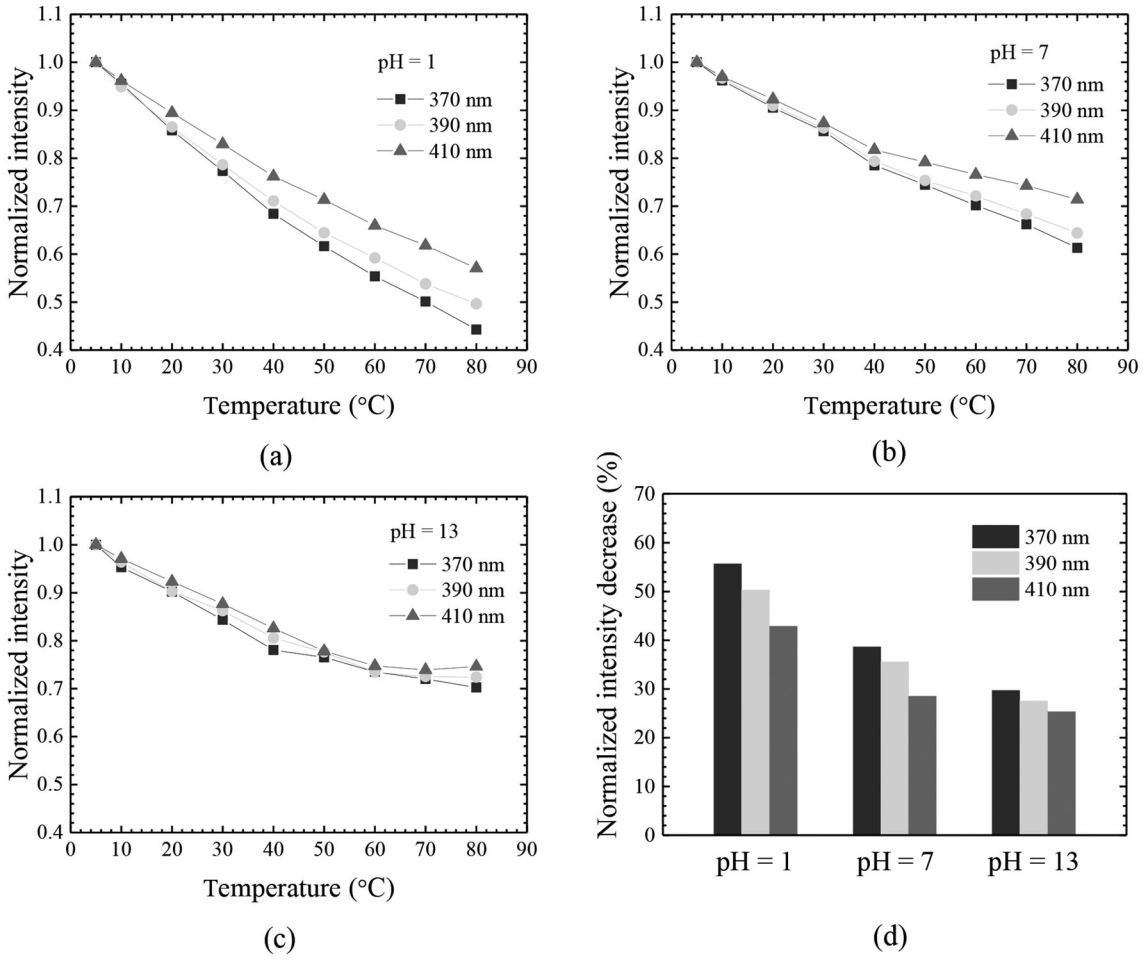

Fig. 4. (a)–(c) Temperature dependence of fluorescence intensity for three excitation wavelengths of different pH value; (d) the normalized intensity reduction for the temperature range of 75°C of all of the excitation wavelengths decreases as pH value increases from pH = 1 to pH = 13. But all of them are very significant when compared with traditional semiconductor QDs.

wavelength is 410 nm, which is more sensitive than the traditional QDs. As the pH value is increased to pH = 7, the normalized intensity decreases of 370 nm, 390 nm, and 410 nm drop to 39%, 36%, and 29%, respectively. When the pH value becomes 13, the difference between different excitation wavelengths becomes less obvious, and the normalized intensity decreases within the same temperature range become 27%, 25%, and 23%. This temperature-induced intensity decrease can be explained by the increased non-radiative decay rate as temperature rises, thus leading to decreased quantum efficiency [36]. For low pH value cases, more trap sites on the GQDs surface are removed, the non-radiative decay rate increases quickly as temperature increases, and it leads to a more significant intensity decrease. For alkaline environment (pH = 13), the decrease of non-radiative decay rate becomes slow and leads to a relatively weaker intensity decrease. It is worth noting that for all pH values, the intensity decrease rates (23% to 56%) are more significant compared with traditional semiconductor QDs within this small temperature range [29, 31, 32], indicating GQDs is effective temperature markers.

The temperature dependence of peak wavelength in the fluorescence spectrum is another important feature in temperature measurements. It is the intrinsic property of many materials stemming from the elastic and non-elastic photon scattering. Temperature of to-be-measured material can be readily determined from the measured frequency/wavelength of scattered/emitted light. For GQDs, one problem is that the fluorescence spectrum is broad and asymmetric, which makes it difficult for using the traditional

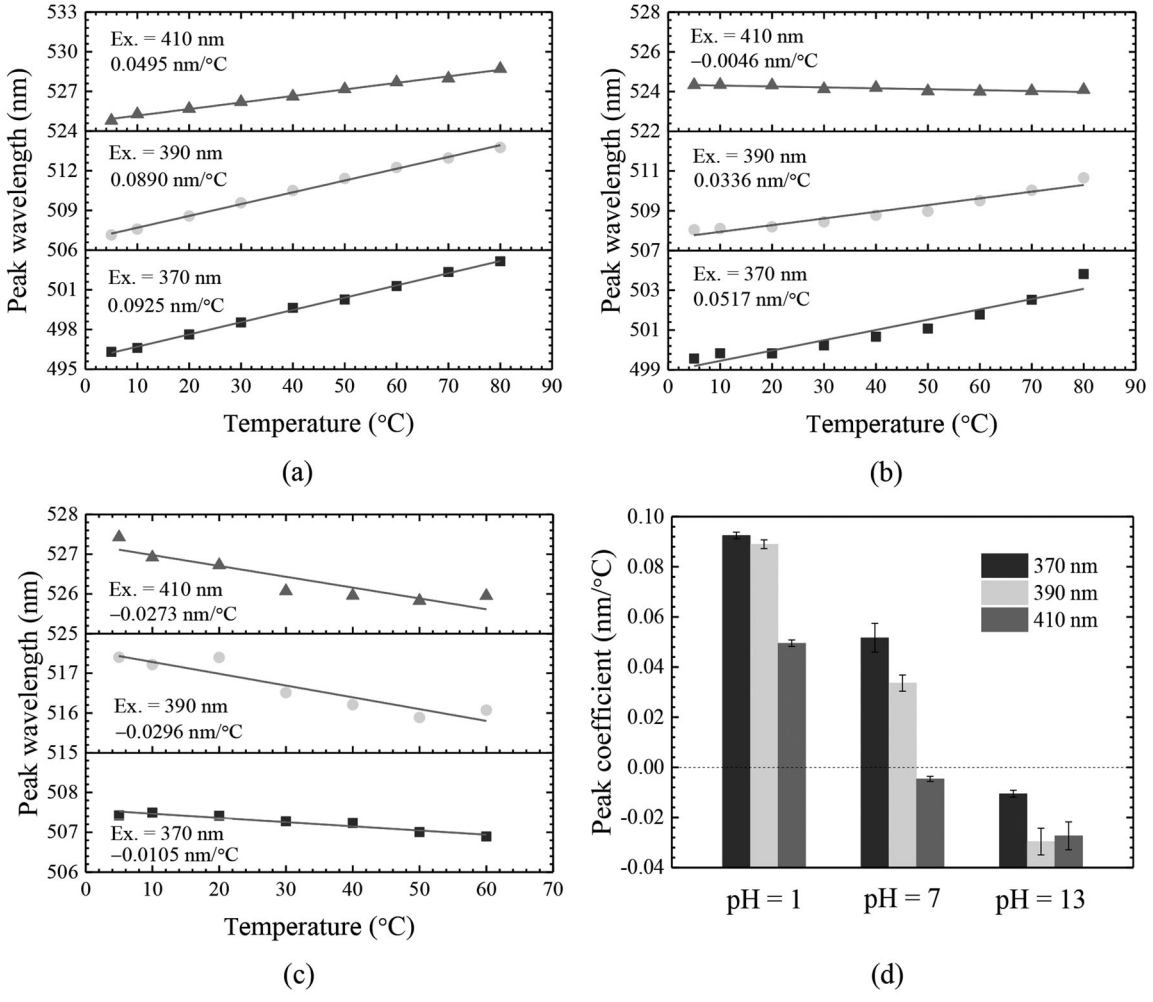

Fig. 5. Temperature dependence of peak position for different excitation wavelengths of pH = 1 (a), pH = 7 (b), and pH = 13 (c). Linear fittings (red solid lines) of the experimental results (solid dots) show that the peak positions of all the spectra have a good linear relationship with temperature; (d) the temperature coefficients for all the wavelengths decrease as pH value increases. When pH = 13, the temperature coefficients switch from positive to negative (as the fluorescence spectrum of 70°C and 80°C in pH = 13 are rough and overlap, these data were omitted).

Gaussian and Lorentz functions to fit peak positions. Instead, we developed a method by defining the "theoretical" peak position on 1/2 x-axial value of 1/2 integration area of the peak in our previous work [36]. Figures 5a–5c show the peak shifts of different pH values for the temperature range and excitation wavelengths. All the spectrum peak positions show a well linear relationship with temperature. Figure 5d lists the summary of all the temperature coefficients under different excitation wavelengths and different pH values. When pH = 1 (Fig. 5a), the temperature coefficients for excitation wavelength of 370, 390, and 410 nm are 0.0925 nm/°C, 0.0890 nm/°C, and 0.0495 nm/°C, respectively. From Fig. 5d, it is found that the temperature coefficients of the peak wavelength decrease as the pH value is increased, gradually from positive to negative (red shift to blue shift). The reason could be that as the pH value is increased, the GQDs surface modification and the change of the zigzag edge sites make the GQDs agglomerate, as reported in previous studies [51, 55]. When the size of GQDs in the alkaline environment becomes larger, the temperature-induced band gap of the GQDs varies [38], thus leading to the blue shift of the GQDs in the high pH value. As of course, the temperature coefficients of different excitation wavelengths are different, as shown in Fig. 5d. For example, the temperature coefficients of 370 nm in pH = 1, pH = 7, and pH = 13 are 0.0925 nm/°C, 0.0517 nm/°C, and −0.0105 nm/°C, respectively. For excitation wavelengths of 390 and 410 nm, similar trends can be found, but the values become smaller.

Figure 6 shows the temperature dependence of peak width under different excitation wavelengths and

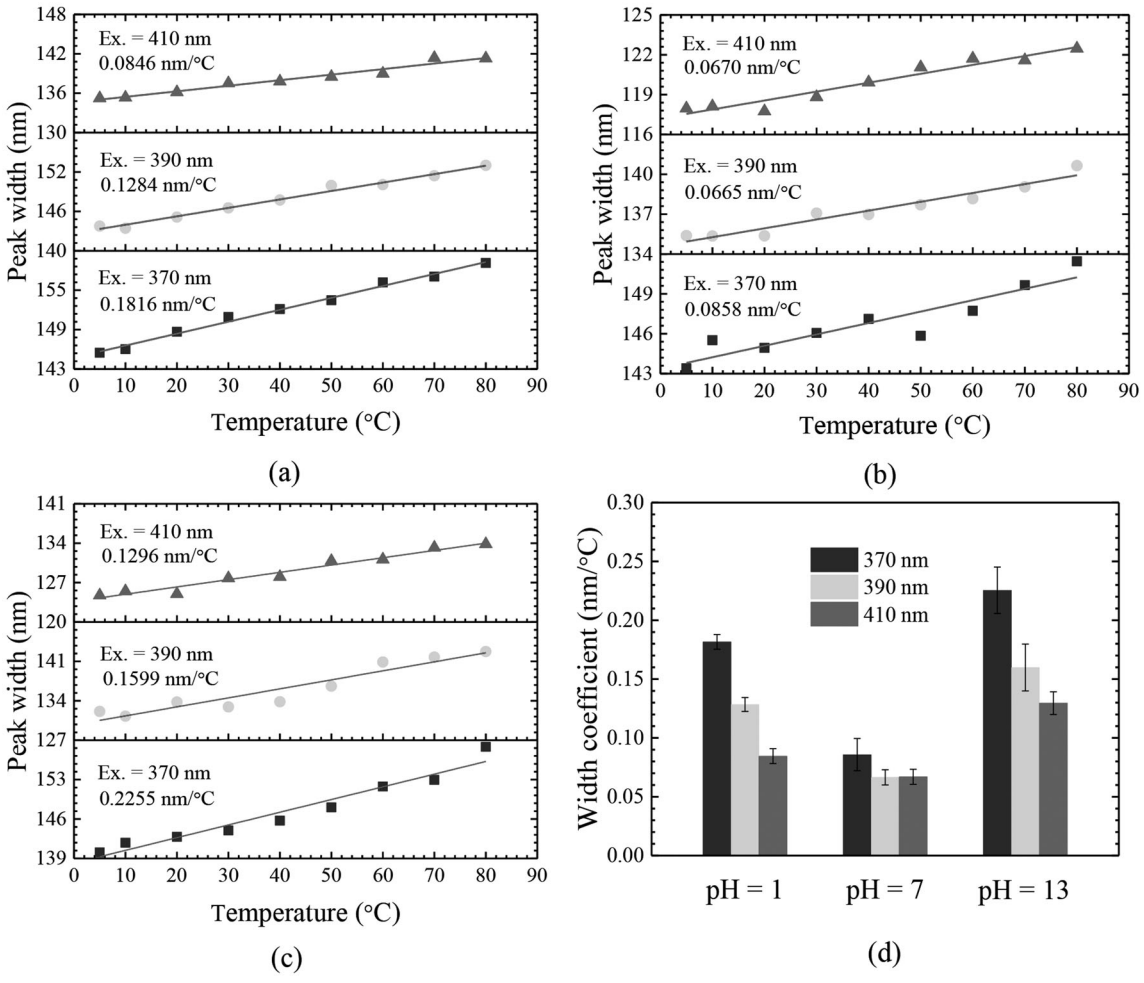

Fig. 6. Temperature dependence of peak width for different excitation wavelengths of pH = 1 (a), pH = 7 (b), and pH = 13 (c). Peak width shows a good linear relationship with temperature (red solid lines are linear fitting of experimental results); (d) the summary of all the temperature coefficients of peak width under different excitation wavelengths and different pH values, which are larger when compared with the peak position temperature coefficients in the same conditions.

different pH values. The width is defined at the point when fluorescence intensity equals the half of the maximum as the full width at half maximum (FWHM) [36]. Through linear fitting, it is found that the temperature coefficients of peak width are larger when comparing with the peak position temperature coefficients in the same conditions. This reveals that it could be another effective feature for temperature probing. As seen from Fig. 6d, both excitation wavelength and pH-value have influence on the thermal coefficient. For example, for excitation wavelength of 370 nm, the temperature coefficients vary from 0.1816 nm/°C to 0.0858 nm/°C, then to 0.2255 nm/°C as pH value is changed from pH = 1 to pH = 7, and then to pH = 13. As the excitation wavelength is changed to 390 nm, the temperature coefficients for pH = 1, pH = 7, and pH = 13 are 0.1284 nm/°C, 0.0665 nm/°C, and 0.1599 nm/°C, respectively. And for excitation wavelength of 410 nm, corresponding temperature coefficients are 0.0846 nm/°C, 0.067 nm/°C, and 0.1296 nm/°C, respectively.

The above summary of the temperature dependence of fluorescence intensity, peak wavelength and width indicates that it is very important to choose the most appropriate excitation wavelength and the best optical features of the fluorescence spectrum when using GQDs to measure temperature in the environment of different pH value. For complex environments, especially in biology field when probing living vivo cells, the GQD is an excellent candidate for its superior biocompatibility and extremely low cytotoxicity. The excellent fluorescence response of GQDs under a low pH value makes it more favorable to the acid environment in most living cells. As discussed above, the lower excitation wavelength closing to the absorption band is more sensitive and should be selected. Temperature-induced intensity decrease keeps significant for all pH values. This reveals that using fluorescence intensity for sensing temperature is the first option in most cases. Since temperature coefficients of peak position are stronger in acidic conditions than those in neutral and alkaline conditions, this could be another option for temperature determination. The temperature coefficients of width are found strong in acidic and alkaline conditions, but weak when in neutral condition. This reveals that when treating temperature coefficients of peak width, caution should be made on both the excitation wavelengths and pH values. When doing bio-thermal measurements using GQDs, pH value should be considered to choose the best temperature-dependent optical properties for temperature calibration. For example, when measuring a stomach tissue/cell where pH value is strongly acid, our study shows that peak intensity, peak wavelength and peak width are all sensitive to temperature, and shorter excitation wavelength should be chosen. But for blood or mouth cells, where pH value is near neutral, fluorescence intensity can give better temperature information.

4. CONCLUSIONS

When applying the GQDs for nanoscale thermometry, it needs to be notified that not just excitation wavelength but also the pH value of the environment condition determine the quantum efficiency of the fluorescence excitation. In this work, the different temperature dependence of fluorescence spectroscopy of GQDs caused by pH value is studied combined at different excitation wavelengths. The normalized peak intensity ranges from 56% to 30% in the decreasing trend within the temperature range of 75°C as the pH value is increased from pH = 1 to pH = 13 for all wavelengths of 370, 390, and 410 nm. The temperature coefficient of peak position (wavelength) is strongly dependent on the pH values: when the pH value increases from acid to alkaline condition, the temperature coefficients turn from positive to negative (red shift to blue shift). The largest temperature coefficients of peak width 0.2255 nm/°C is observed for a wavelength of 370 nm in pH = 13, indicating that the peak width can be used as the reference for temperature determination. As GQDs are good temperature markers in a bio-thermal field, this study can benefit the selection of nanoscale thermal probe to improve measurement accuracy for temperature calibration.

ACKNOWLEDGMENTS

This work was supported by the National Natural Science Foundation of China (grant no. 51576145) and by the China Postdoctoral Science Foundation (grant no. 2017M622928).

REFERENCES

1. Brus, L.E., A Simple Model for the Ionization Potential, Electron Affinity, and Aqueous Redox Potentials of Small Semiconductor Crystallites, *J. Chem. Phys.*, 1983, vol. 79, no. 11, pp. 5566–5571.
2. Leutwyler, W.K., Bürgi, S.L., and Burgl, H., Semiconductor Clusters, Nanocrystals, and Quantum Dots, *Science*, 1996, vol. 271, no. 5251, pp. 933–937.
3. Ponomarenko, L.A., Schedin, F., Katsnelson, M.I., Yang, R., Hill, E.W., Novoselov, K.S., and Geim, A.K., Chaotic Dirac Billiard in Graphene Quantum Dots, *Science*, 2008, vol. 320, no. 5874, pp. 356–358.
4. Reiss, P., Protière, M., and Li, L., Core/Shell Semiconductor Nanocrystals, *Small*, 2009, vol. 5, no. 2, pp. 154–168.
5. Bacon, M., Bradley, S.J., and Nann, T., Graphene Quantum Dots, *Part. Part. Syst. Char.*, 2014, vol. 31, no. 4, pp. 415–428.
6. Tyrakowski, C.M. and Snee, P.T., A Primer on the Synthesis, Water-Solubilization and Functionalization of Quantum Dots, Their Use as Biological Sensing Agents, and Present Status, *Phys. Chem. Chem. Phys.*, 2014, vol. 16, no. 3, pp. 837–855.
7. Xue, Q., Huang, H., Wang, L., Chen, Z., Wu, M.H., Li, Z., and Pan, D.Y., Nearly Monodisperse Graphene Quantum Dots Fabricated by Amine-Assisted Cutting and Ultrafiltration, *Nanoscale*, 2013, vol. 5, no. 24, pp. 12098–12103.
8. Medintz, I.L., Uyeda, H.T., Goldman, E.R., and Mattoussi, H., Quantum Dot Bioconjugates for Imaging, Labeling and Sensing, *Nat. Mater.*, 2005, vol. 4, no. 6, pp. 435–446.
9. Michalet, X., Pinaud, F.F., Bentolila, L.A., Tsay, J.M., Doose, S., Li, J.J., Sundaresan, G., Wu, A.M., Gambhir, S.S., and Weiss, S., Quantum Dots for Live Cells, in Vivo Imaging, and Diagnostics, *Science*, 2005, vol. 307, no. 5709, pp. 538–544.
10. Zhu, S.J., Zhang, J.H., Qiao, C.Y., Tang, S.J., Li, Y.F., Yuan, W.J., Li, B., Tian, L., Liu, F., Hu, R., Gao, H.N., Wei, H.T., Zhang, H., Sun, H.C., and Yang, B., Strongly Green-Photoluminescent Graphene Quantum Dots for Bioimaging Applications, *Chem. Commun.*, 2011, vol. 47, no. 24, pp. 6858–6860.
11. Pan, D.Y., Guo, L., Zhang, J.C., Xi, C., Xue, Q., Huang, H., Li, J.H., Zhang, Z.W., Yu, W.J., Chen, Z.W., Li, Z., and Wu, M.H., Cutting Sp2 Clusters in Graphene Sheets into Colloidal Graphene Quantum Dots with Strong Green Fluorescence, *J. Mater. Chem.*, 2012, vol. 22, no. 8, pp. 3314–3318.
12. Zhang, L.M., Xing, Y.D., He, N.Y., Zhang, Y., Lu, Z.X., Zhang, J.P., and Zhang, Z.J., Preparation of Graphene Quantum Dots for Bioimaging Application, *J. Nanosci. Nanotech.*, 2012, vol. 12, no. 3, pp. 2924–2928.
13. Schaller, R.D. and Klimov, V.I., High Efficiency Carrier Multiplication in PbSe Nanocrystals: Implications for Solar Energy Conversion, *Phys. Rev. Lett.*, 2004, vol. 92, no. 18, p. 186601.
14. Koleilat, G.I., Levina, L., Shukla, H., Myrskog, S.H., Hinds, S., Pattantyus-Abraham, A.G., and Sargent, E.H., Efficient, Stable Infrared Photovoltaics Based on Solution-Cast Colloidal Quantum Dots, *ACS Nano*, 2008, vol. 2, no. 5, pp. 833–840.
15. Guo, C.X., Yang, H.B., Sheng, Z.M., Lu, Z.S., Song, Q.L., and Li, C.M., Layered Graphene/Quantum Dots for Photovoltaic Devices, *Angew. Chem. Int. Ed.*, 2010, vol. 49, no. 17, pp. 3014–3017.
16. Yan, X., Cui, X., Li, B., and Li, L.S., Large Solution-Processable Graphene Quantum Dots as Light Absorbers for Photovoltaics, *Nano Lett.*, 2010, vol. 10, no. 5, pp. 1869–1873.
17. Gupta, V., Chaudhary, N., Srivastava, R., Sharma, G.D., Bhardwaj, R., and Chand, S., Luminscent Graphene Quantum Dots for Organic Photovoltaic Devices, *J. Am. Chem. Soc.*, 2011, vol. 133, no. 26, pp. 9960–9963.
18. Li, Y., Hu, Y., Zhao, Y., Shi, G.Q., Deng, L., Hou, Y.B., and Qu, L.T., An Electrochemical Avenue to Green-Luminescent Graphene Quantum Dots as Potential Electron-Acceptors for Photovoltaics, *Adv. Mater.*, 2011, vol. 23, no. 6, pp. 776–780.
19. Shen, J.H., Zhu, Y.H., Yang, X.L., Zong, J., Zhang, J.M., and Li, C.Z., One-Pot Hydrothermal Synthesis of Graphene Quantum Dots Surface-Passivated by Polyethylene Glycol and Their Photoelectric Conversion under Near-Infrared Light, *New J. Chem.*, 2012, vol. 36, no. 1, pp. 97–101.
20. Ip, A.H., Thon, S.M., Hoogland, S., Voznyy, O., Zhitomirsky, D., Debnath, R., Levina, L., Rollny, L.R., Carey, G.H., Fischer, A., Kemp, K.W., Kramer, I.J., Ning, Z., Labelle, A.J., Chou, K.W., Amassian, A., and Sargent, E.H., Hybrid Passivated Colloidal Quantum Dot Solids, *Nat. Nanotech.*, 2012, vol. 7, no. 9, pp. 577–582.
21. Ran, X., Sun, H.J., Pu, F., Ren, J.S., and Qu, X.G., Ag Nanoparticle-Decorated Graphene Quantum Dots for Label-Free, Rapid and Sensitive Detection of Ag^+ and Biothiols, *Chem. Commun.*, 2013, vol. 49, no. 11, pp. 1079–1081.
22. Wang, F.X., Gu, Z.Y., Lei, W., Wang, W.J., Xia, X.F., and Hao, Q.L., Graphene Quantum Dots as a Fluorescent Sensing Platform for Highly Efficient Detection of Copper(II) Ions, *Sensor. Actuat. B-Chem.*, 2014, vol. 190, pp. 516–522.
23. Snee, P.T., Somers, R.C., Nair, G., Zimmer, J.P., Bawendi, M.G., and Nocera, D.G., A Ratiometric CdSe/ZnS Nanocrystal pH Sensor, *J. Am. Chem. Soc.*, 2006, vol. 128, no. 41, pp. 13320/13321.

24. Frasco, M.F. and Chaniotakis, N., Semiconductor Quantum Dots in Chemical Sensors and Biosensors, *Sensors*, 2009, vol. 9, no. 9, pp. 7266–7286.
25. Shi, J.Y., Chan, C.Y., Pang, Y., Ye, W.W., Tian, F., Lyu, J., Zhang, Y., and Yang, M., A Fluorescence Resonance Energy Transfer (FRET) Biosensor Based on Graphene Quantum Dots (GQDs) and Gold Nanoparticles (AuNPs) for the Detection of MecA Gene Sequence of Staphylococcus Aureus, *Biosens. Bioelectron.*, 2014, vol. 67, no. 5, pp. 595–600.
26. Wu, Z.L., Gao, M.X., Wang, T.T., Wan, X.Y., Zheng, L.L., and Huang, C.Z., A General Quantitative pH Sensor Developed with Dicyandiamide N-Doped High Quantum Yield Graphene Quantum Dots, *Nanoscale*, 2014, vol. 6, no. 7, pp. 3868–3874.
27. Dai, Y.T., Fan, J.C., Chen, Y.F., Lin, R.M., Lee, S.C., and Lin, H.H., Temperature Dependence of Photoluminescence Spectra in InAs/GaAs Quantum Dot Superlattices with Large Thicknesses, *J. Appl. Phys.*, 1997, vol. 82, no. 9, pp. 4489–4492.
28. Walker, G.W., Sundar, V.C., Rudzinski, C.M., Wun, A.W., Bawendi, M.G., and Nocera, D.G., Quantum-Dot Optical Temperature Probes, *Appl. Phys. Lett.*, 2003, vol. 83, no. 17, pp. 3555–3557.
29. Al Salman, A., Tortschanoff, A., Mohamed, M., Tonti, D., Van Mourik, F., and Chergui, M., Temperature Effects on the Spectral Properties of Colloidal CdSe Nanodots, Nanorods, and Tetrapods, *Appl. Phys. Lett.*, 2007, vol. 90, no. 9, p. 093104.
30. Yue, Y.N. and Wang, X.W., Nanoscale Thermal Probing, *Nano Rev.*, 2012, vol. 3, p. 11586.
31. Li, S., Zhang, K., Yang, J.M., Lin, L.W., and Yang, H., Single Quantum Dots as Local Temperature Markers, *Nano Lett.*, 2007, vol. 7, no. 10, pp. 3102–3105.
32. Gu, P.F., Zhang, Y., Feng, Y., Zhang, T.Q., Chu, H.R., Cui, T., Wang, Y.D., Zhao, J., and William, W.Y., Real-Time and On-Chip Surface Temperature Sensing of GaN LED Chips Using PbSe Quantum Dots, *Nanoscale*, 2013, vol. 5, no. 21, pp. 10481–10486.
33. Yue, Y.N., Zhang, J.C., Xie, Y.S., Chen, W., and Wang, X.W., Energy Coupling across Low-Dimensional Contact Interfaces at the Atomic Scale, *Int. J. Heat Mass Transfer*, 2017, vol. 110, pp. 827–844.
34. Wan, X., Li, C.Z., Yue, Y.N., Xie, D.M., Xue, M.X., and Hu, N.S., Development of Steady-State Electrical-Heating Fluorescence-Sensing (SEF) Technique for Thermal Characterization of One-Dimensional (1D) Structures by Employing Graphene Quantum Dots (GQDs) as Temperature Sensors, *Nanotech.*, 2016, vol. 27, no. 44, p. 445706.
35. Wu, H., Cai, K., Zeng, H.T., Zhao, W.S., Xie, D.M., Yue, Y.N., Xiong, Y.H., and Zhang, X., Time-Domain Transient Fluorescence Spectroscopy for Thermal Characterization of Polymers, *Appl. Therm. Eng.*, 2018, vol. 138, pp. 403–408.
36. Li, C.Z. and Yue, Y.N., Fluorescence Spectroscopy of Graphene Quantum Dots: Temperature Effect at Different Excitation Wavelengths, *Nanotech.*, 2014, vol. 25, no. 43, p. 435703.
37. Wang, L., Wang, Y.L., Xu, T., Liao, H.B., Yao, C.J., Liu, Y., Li, Z.W., Chen, Z.W., Pan, D.Y., and Sun, L.T., Gram-Scale Synthesis of Single-Crystalline Graphene Quantum Dots with Superior Optical Properties, *Nat. Commun.*, 2014, vol. 5, pp. 5357–5365.
38. Dai, Q.Q., Zhang, Y., Wang, Y.N., Hu, M.Z., Zou, B., Wang, Y.D., and Yu, W.W., Size-Dependent Temperature Effects on PbSe Nanocrystals, *Langmuir*, 2010, vol. 26, no. 13, pp. 11435–11440.
39. Joshi, A., Narsingi, K., Manasreh, M., Davis, E., and Weaver, B., Temperature Dependence of the Band Gap of Colloidal CdSe/ZnS Core/Shell Nanocrystals Embedded into an Ultraviolet Curable Resin, *Appl. Phys. Lett.*, 2006, vol. 89, no. 13, p. 131907.
40. Sanchez-Ruiz, J.M., Protein Kinetic Stability, *Biophys. Chem.*, 2010, vol. 148, no. 148, pp. 1–15.
41. Suzuki, M., Tseeb, V., Oyama, K., and Ishiwata, S., Microscopic Detection of Thermogenesis in a Single HeLa Cell, *Biophys. J.*, 2007, vol. 92, no. 6, pp. L46–L48.
42. Chapman, C., Liu, Y., Sonek, G., and Tromberg, B., The Use of Exogenous Fluorescent Probes for Temperature Measurements in Single Living Cells, *Photochem. Photobiol.*, 1995, vol. 62, no. 3, pp. 416–425.
43. Vetrone, F., Naccache, R., Zamarron, A., Juarranz de la Fuente, A., Sanz-Rodriguez, F., Martinez Maestro, L., Martin Rodriguez, E., Jaque, D., Garcia Solé, J., and Capobianco, J.A., Temperature Sensing Using Fluorescent Nanothermometers, *ACS Nano*, 2010, vol. 4, no. 6, pp. 3254–3258.
44. Yang, J.M., Yang, H., and Lin, L.W., Quantum Dot Nano Thermometers Reveal Heterogeneous Local Thermogenesis in Living Cells, *ACS Nano*, 2011, vol. 5, no. 6, pp. 5067–5071.
45. Donner, J.S., Thompson, S.A., Kreuzer, M.P., Baffou, G., and Quidant, R., Mapping Intracellular Temperature Using Green Fluorescent Protein, *Nano Lett.*, 2012, vol. 12, no. 4, pp. 2107–2111.
46. Okabe, K., Inada, N., Gota, C., Harada, Y., Funatsu, T., and Uchiyama, S., Intracellular Temperature Imaging with a Fluorescent Polymeric Thermometer and Fluorescence Lifetime Imaging Microscopy, *Nat. Commun.*, 2012, vol. 25, no. 2, pp. 23–25.
47. Kucsko, G., Maurer, P., Yao, N., Kubo, M., Noh, H., Lo, P., Park, H., and Lukin, M., Nanometre-Scale Thermometry in a Living Cell, *Nature*, 2013, vol. 500, no. 7460, pp. 54–58.

48. Tomasulo, M., Yildiz, I., and Raymo, F.M., pH-sensitive Quantum Dots, *J. Phys. Chem. B*, 2006, vol. 110, no. 9, pp. 3853–3855.
49. Deng, Z.T., Zhang, Y., Yue, J.C., Tang, F.Q., and Wei, Q., Green and Orange CdTe Quantum Dots as Effective pH-sensitive Fluorescent Probes for Dual Simultaneous and Independent Detection of Viruses, *J. Phys. Chem. B*, 2007, vol. 111, no. 41, pp. 12024–12031.
50. Liu, Y.S., Sun, Y., Vernier, P.T., Liang, C.H., Chong, S.Y.C., and Gundersen, M.A., pH-sensitive Photoluminescence of CdSe/ZnSe/ZnS Quantum Dots in Human Ovarian Cancer Cells, *J. Phys. Chem. C*, 2007, vol. 111, no. 7, pp. 2872–2878.
51. Yang, F., Zhao, M.L., Zheng, B.Z., Xiao, D., Wu, L., and Guo, Y., Influence of pH on the Fluorescence Properties of Graphene Quantum Dots Using Ozonation Pre-Oxide Hydrothermal Synthesis, *J. Mater. Chem.*, 2012, vol. 22, no. 48, pp. 25471–25479.
52. Liu, R.L., Wu, D.Q., Feng, X.L., and Mullen, K., Bottom-Up Fabrication of Photoluminescent Graphene Quantum Dots with Uniform Morphology, *J. Am. Chem. Soc.*, 2011, vol. 133, no. 39, pp. 15221–15223.
53. Shen, J.H., Zhu, Y.H., Yang, X.L., and Li, C.Z., Graphene Quantum Dots: Emergent Nanolights for Bioimaging, Sensors, Catalysis and Photovoltaic Devices, *Chem. Commun.*, 2012, vol. 48, no. 31, pp. 3686–3699.
54. Gao, M., Kirstein, S., Möhwald, H., Rogach, A.L., Kornowski, A., Eychmüller, A., and Weller, H., Strongly Photoluminescent CdTe Nanocrystals by Proper Surface Modification, *J. Phys. Chem. B*, 1998, vol. 102, no. 43, pp. 8360–8363.
55. Zhang, H., Zhou, Z., Yang, B., and Gao, M.Y., The Influence of Carboxyl Groups on the Photoluminescence of Mercaptocarboxylic Acid-Stabilized CdTe Nanoparticles, *J. Phys. Chem. B*, 2002, vol. 107, no. 1, pp. 8–13.